원형관에서의 음해법을 이용한 3차원 비압축성 부정류 흐름에 관한 수치모의

Three Dimensional Incompressible Unsteady Flows in a Circular Tube Using the Navier-Stokes Equations With Beam and Warming Method

박기두*, 이길성**, 성진영***
Kidoo Park, Kil Seong Lee, Jinyoung Sung

Abstract

The governing equations in generalized curvilinear coordinates for a 3D pulsatile flow are the Incompressible Navier-Stokes (INS) equations with the artificial dissipative terms and continuity equation discretized using a second-order accurate, finite volume method on the nonstaggered computational grid. This method adopts a dual or pseudo time-stepping Artificial Compressibility (AC) method integrated in pseudo-time. The computational technique implements the implicit approximate factorization method of the Beam and Warming method (1978), which is the extension of the Alternate Direction Implicit (ADI) method. The algorithm yields practically identical velocity profiles and secondary flows that are in excellent overall agreement with an experimental measurement (Rindt & Steenhoven, 1991).

Keywords: Incompressible Navier Stokes Equations, Generalized Curvilinear Coordinates, Artificial Compressibility Algorithms, Artificial Dissipative Terms, Beam and Warning Method, Alternate Direction Implicit

1. Introduction

Computational Fluid Dynamics (CFD) method widely deals with the variety of engineering applications; a numerical method has developed to simulate the various unsteady problems such as the simulations of river hydraulics including natural river channels with complex hydraulic structures such as bridge piers, abutments, and complexity of flow in a meandering channel and cardiovascular fluid mechanics called blood flows. CFD methods can predict and evaluate quantities of complex engineering flow situations according to Reynolds numbers. The main challenges of CFD method in the accurate simulation of complex engineering flows originate from various geometric complexities and the physics of flow. It is important objective of this study to contribute to the application and validation of the unsteady simulations. To evaluate

* 서울대학교 공과대학 건설환경공학부 박사과정 · E-mail : hydrol88@snu.ac.kr

** 정회원·서울대학교 공과대학 건설환경공학부 교수·E-mail : kilselee@snu.ac.kr

*** 서울대학교 공과대학 건설환경공학부 석사과정 · E-mail : blackleo83@snu.ac.kr

this numerical ability of the method to simulate flows, we apply it to compute pulsatile flow in a circular tube with strong curvature. The test case (Rindt & Steenhoven, 1991) is chosen to demonstrate the efficiency and the accuracy of this method in a complex 3D pulsatile flow.

2. Governing Equations

The governing equations in generalized curvilinear coordinates, using dual or pseudo time-stepping Artificial Compressibility (AC) method to couple pressure and velocities, are the three-dimensional, incompressible Navier-Stokes (NS) equations and continuity equation, nondimensionlized by ρ, U_o, and L_o. The governing equations follow

$$\Gamma\frac{\partial Q}{\partial t}+J\frac{\partial}{\partial t}(F^l-F_\nu^l)=0, \tag{1}$$

$$\Gamma=diag(0,\,1,\,1,\,1),$$

$$Q=(p,\,u_1,u_2,\,u_3)^T,$$

$$F^{\,l}=\frac{1}{J}(U^l,\;u_1U^l+p\xi_{x_1}^l,u_2U^l+p\xi_{x_2}^l,\;u_3U^l+p\xi_{x_3}^l),$$

$$F_\nu^l=\frac{1}{JRe}\left(0,\,g^{ml}\frac{\partial u_1}{\partial\xi^m},\,g^{ml}\frac{\partial u_2}{\partial\xi^m},\,g^{ml}\frac{\partial u_3}{\partial\xi^m}\right)^T,$$

where x_l are the Cartesian coordinates x, y, and z. ξ^l are curvilinear coordinates ξ, η, and ζ, respectively, $\xi_{x_m}^l$ are the metrics of the geometric transformation, g^{ml} are the components of the contravariant metric tensor, and J is the Jacobian of the geometric transformation. U^l are the contravariant velocity components, $U^l=u_m\xi_{x_l}^m$, u_m are the Cartesian velocity components, and u, v, and w, and p is the static pressure divided by the density. Finally, Re is the Reynolds number of the flow, which is based on characteristic length and velocity scales and the kinematic viscosity of the fluid.

The governing equations are discretized in strong conservation form using a three-point backward, second order accurate Euler implicit scheme for the temporal derivative and three-point, second order accurate central differencing for the spatial derivatives,

$$\Gamma\frac{1}{J}\left(\frac{dQ}{dt}\right)_{i,j,k}+\left(\delta_{\xi^l}\tilde{F}^l+\delta_{\xi^l}\tilde{F}_\nu^l\right)_{i,j,k}^{n+1}=0 \tag{2}$$

where $\delta_{\xi^1}(\;)_{i,j,k}=\dfrac{(\;)_{i+1/2,j,k}-(\;)_{i-1/2,j,k}}{\triangle\xi^1}$.

The flux $\tilde{F}$ is the flux F at the cell interfaces and D is the artificial dissipation flux, especially, the matrix valued scheme (Lin and Sotiropoulos, 1997),

$$\tilde{F}_{i+1/2,j,k}^1=\frac{1}{2}\left(F_{i,j,k}^1+F_{i+1,j,k}^1\right)+D_{i+1/2,j,k}^1 \tag{3}$$

$$D_{i+1/2,j,k}^1=\epsilon\delta_{\xi^1}\left(|A^{\,1}|\delta_{\xi^1}\delta_{\xi^1}\right)Q_{i+1/2,j,k} \tag{4}$$

where ϵ is a constant, $|A^l|$ is the absolute value of the Jacobian matrix $A^l = \partial F^l / \partial Q$.

3. Numerical Methods

The governing equations are discretized in strong conservation form using a second order accurate finite volume method on a non-staggered grid. To enhance the efficiency and robustness of the algorithm, we can implement the local dual time stepping and the implicit method of the Beam and Warming method which is the extension of the ADI method.

The discrete dual-time equations can be written as follows,

$$\frac{1}{J}\left(\frac{\triangle Q_{i,j,k}}{\triangle \tau} + \Gamma \frac{2}{3}\frac{\triangle Q_{i,j,k}}{\triangle t}\right) = -\Gamma \frac{1}{J}\frac{3Q^l_{i,j,k} - 4Q^n_{i,j,k} + Q^{n-1}_{i,j,k}}{2\triangle t} - \left(\delta_{\xi^m}\tilde{F}^m - \delta_{\xi^m}\tilde{F}^m_v\right)^{l+1}_{i,j,k} \quad (5)$$

where $\triangle Q_{i,j,k} = Q^{l+1}_{i,j,k} - Q^l_{i,j,k}$

The linearization in pseudo-time is as follows,

$$\frac{1}{J}\left[\left(\frac{1}{\triangle \tau} + \Gamma \frac{2}{3}\frac{1}{\triangle t}\right) I + \pounds^l\right] \triangle Q_{i,j,k} \quad (6)$$

$$= -\Gamma \frac{1}{J}\frac{3Q^l_{i,j,k} - 4Q^n_{i,j,k} + Q^{n-1}_{i,j,k}}{2\triangle t} - \left(\delta_{\xi^m}\tilde{F}^m - \delta_{\xi^m}\tilde{F}^m_v\right)^l_{i,j,k}$$

where $\pounds^l$ is the Jacobian of the spatial residual in the right hand side (R) of equation (5), $\pounds = \partial R / \partial Q$. The resulting equation is approximated by the following approximate factorization,

$$\left[D^l + \pounds^l_1\right][D^l]^{-1}\left[D^l + \pounds^l_2\right][D^l]^{-1}\left[D^l + \pounds^l_3\right][D^l]^{-1} \triangle Q^l = -R(Q^l) \quad (7)$$

where $D^l = \left(\frac{1}{\triangle \tau} + \Gamma \frac{3}{2}\frac{1}{\triangle t}\right) I$, and $\pounds^l_m = \delta_{\xi^m}\left(\frac{\partial \tilde{F}^m}{\partial Q} + \frac{\partial \widetilde{F^m_v}}{\partial Q}\right)$.

Equation (7) can be solved through a three step procedure each one involving the inversion of a block tridiagonal system,

$$\left[D^l + \pounds^l_1\right] \triangle Q^* = -R(Q^l) \quad (8)$$

$$\left[D^l + \pounds^l_2\right] \triangle Q^{**} = D^l \triangle Q^*$$

$$\left[D^l + \pounds^l_3\right] \triangle Q = D^l \triangle Q^{**}$$

$$Q^{l+1} = Q^l + \triangle Q.$$

The local time step is computed at each grid,

$$\triangle \tau = \min\left[\frac{\mathrm{CFL}}{\max\left(\lambda_{\xi^1}, \lambda_{\xi^2}, \lambda_{\xi^3}\right)}, \frac{\mathrm{VN}}{\frac{1}{\mathrm{Re}}\max\left(g^{11}, g^{22}, g^{33}\right)}\right] \quad (9)$$

where λ_ξ is the spectral radius of the Jacobian matrices, CFL is the Courant-Friedrich-Lewis number and VN is the von Neumann number.

4. Results and Conclusion

The numerical solution is to validate the accuracy of this solver for unsteady flow, especially, the pulsating flow in a circular tube with 90° bend after then, the developed numerical model is applied to simulate blood flows. The simulation of pulsating flow in a curved tube with 90° bend is a more challenging study of the temporal flow condition to evaluate the abilities of the our numerical method. The experimental flow is one of six unsteady flow experiment conducted by Rindt & Steenhoven (1991) using Laser Doppler Velocimeter (LDV).

The pulsating flows are generated by the combined effects of the a pump that provided a steady flow with $Re = 500$ and a piston pump that introduced a sinusoidal flow variation with a Reynolds number range of the $-300 \leq \mathrm{Re} \leq 300$. Therefore, Reynolds numbers for retrograde and forward flow conditions are 198 and 795, respectively. One cycle of flow pulsations is divided into 32 physical time steps during the calculation with the dimensionless physical time $T = 12.3$ called the period of the incoming flow oscillation.

Boundary conditions are specified at the inlet, outlet, and solid wall boundaries. Inflow boundary conditions are implemented by Dirichlet conditions for the fully developed velocity distribution. No slip and no flux boundary conditions are used on the solid walls. Zero gradient boundary conditions at the outflow boundary and on the symmetry plane (at $z = 0$) are used (Neumann condition). The pressures at all boundaries are obtained by linear extrapolation from interior nodes. Especially, the inlet boundary condition with time is explained as a superposition of steady and unsteady velocity profiles of the pulsating flow given by Eq. (10),

$$u_{unsteady}(r,t) = -\mathrm{i}\frac{K}{\omega}e^{\mathrm{i}\omega t}\left[1-\frac{J_0\left(r\sqrt{\frac{-\mathrm{i}\omega}{\nu}}\right)}{J_0\left(R\sqrt{\frac{-\mathrm{i}\omega}{\nu}}\right)}\right] \tag{10}$$

where J_0 is the Bessel function of the first kind and order zero, R is the radius of the pipe, i is the imaginary unit, and K represents the constant. To evaluate the performance of the implicit method in a 3D flow of a curved 90 degree circular bend, we choose a test case: The finest meshes are $49 \times 41 \times 21$ grid nodes. The CFL number used in this numerical study is CFL = 3.0.

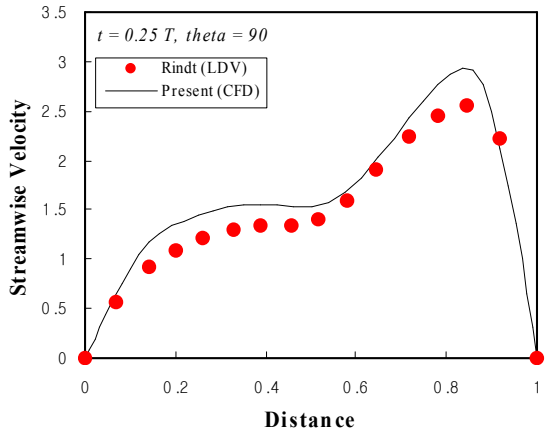

Fig 1. Pulsatile flow at 90° pipe bend at the pulsation cycle *t = 0.25 T*

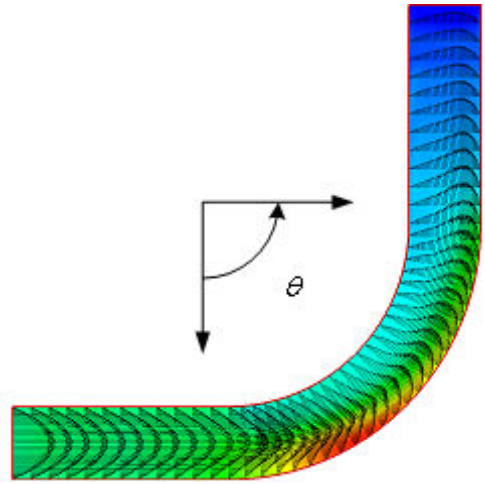

Fig 2. Pulsatile flow at the pulsation cycle *t = 0.25 T*

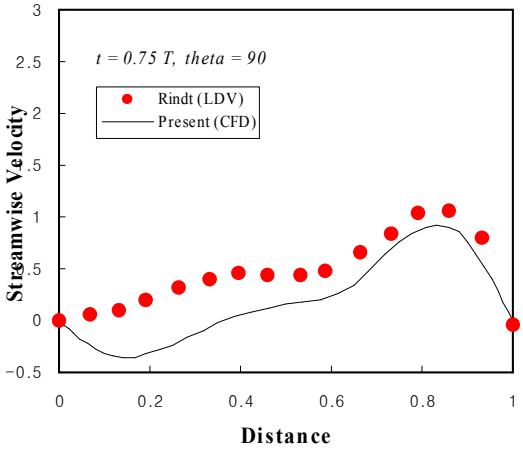

Fig 3. Pulsatile flow at 90° pipe bend at the pulsation cycle *t = 0.75 T*

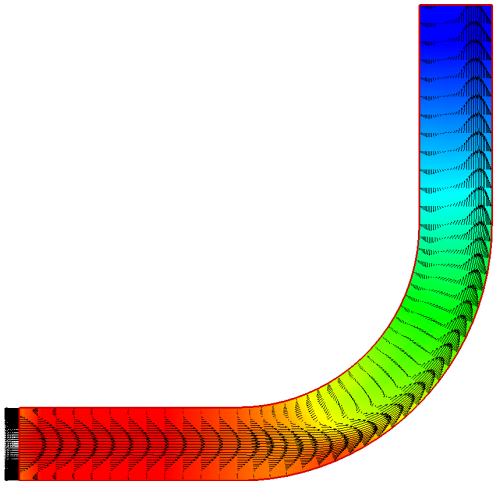

Fig 4. Pulsatile flow at the pulsation cycle *t = 0.75 T*

Acknowledgement

The authors wish to acknowledge the financial support by SNU SIR Group of the BK21 research Program funded by Ministry of Education & Human Resources Development.

References

1. Beam, R. M., and Warming, R .F. (1967). An implicit finite-difference algorithm for hyperbolic systems in conservation-law form, *Journal of Computational Physics*, Vol. 82, No. 2, pp. 87-110.
2. Ge, L., and Sotiropoulos, F. (2005). 3D unsteady RANS Modeling of complex hydraulic engineering flows. I: Numerical model, *Journal of Hydraulic Engineering*, Vol. 131, No. 9, pp.

800-808.
3. Lin, F. B., and Sotiropoulos, F. (1997). Assessment of artificial dissipation models for three-dimensional incompressible flow solutions. *ASME J. Fluids Eng.*, 119(2), pp. 331-340.
4. Park, K., and Lee, K. S. (2007). Numerical simulation of three dimensional incompressible flows using the Navier-Stokes equations with the artificial dissipation terms and a multigrid method, *Proceedings of the Korea Water Resources Association Annual Conference*, pp. 1392-1395.
5. Park, K., and Lee, K. S. (2007). Numerical simulation of unsteady flow in a circular tube with strong curvature using the Navier-Stokes equations, *Proceedings of the Korea Society of Civil Engineers Association Annual Conference*, pp. 4211-4214.
6. Park, K., Lee, K. S., and Kim, K. (2008). Incompressible unsteady Flow in a circular tube using the Navier-Stokes Equations, *The 1st SIR BK21 International Conference on Sustainable Infrastructure*, Seoul, Korea, pp. 146-147.
7. Rindt, C. C. M., and van Steenhoven, A. A. (1991). Unsteady entrance flow in a 90° curved tube, *Journal of Fluid Mechanics*, Vol. 226, pp. 445-474.